Exocyclic coordination of the η^3-fluorenyl, η^3-cyclopenta[*def*]-phenanthrenyl and η^3-8,9-dihydrocyclopenta[*def*]phenanthrenyl anions: X-ray crystal structures, NMR fluxionality and theoretical studies

Maria J. Calhorda,[ab] Isabel S. Gonçalves,[ac] Brian J. Goodfellow,[c] Eberhardt Herdtweck,[d] Carlos C. Romão,*[a] Beatriz Royo[a] and Luís F. Veiros[e]

[a] *Instituto de Tecnologia Química e Biológica, Quinta do Marquês, EAN, Apt 127, 2781-901 Oeiras, Portugal. E-mail: ccr@itqb.unl.pt*
[b] *Departamento de Química e Bioquímica, Faculdade de Ciências, Universidade de Lisboa, 1749-016 Lisboa, Portugal*
[c] *Departamento de Química, Universidade de Aveiro, Campus de Santiago, 3810-193 Aveiro, Portugal*
[d] *Anorganisch-chemisches Institut der Technischen Universität München, Lichtenbergstraße 4, D-85747 Garching bei München, Germany*
[e] *Centro de Química Estrutural, Instituto Superior Técnico, 1049-001 Lisboa Codex, Portugal*

Received (in Montpellier, France) 7th May 2002, Accepted 16th July 2002
First published as an Advance Article on the web 17th October 2002

The novel complexes IndMo(η^3-Flu)$(CO)_2$ (Flu = fluorenyl), (η^5-Ind)Mo(η^3-cpp)$(CO)_2$ (cpp = cyclopenta-[*def*]phenanthrenyl) and (η^5-Ind)Mo(η^3-H_2cpp)$(CO)_2$ (H_2cpp = 8,9-dihydrocyclopenta[*def*]phenanthrenyl) have been prepared and their molecular structures determined. X-Ray crystallographic studies show an *exo*cyclic η^3-coordination for the Flu, cpp and H_2cpp ligands, which is also predicted from DFT calculations. ^{1}H NMR spectra, recorded at temperatures between 303 and 318 K, indicated that exchange broadening was taking place for the protons near the η^3-coordination site. It was found that ring slippage occurred at lower temperatures for Mo-Flu and Mo-H_2cpp than for Mo-cpp. This result is in agreement with the order of the Mo–X bond strengths determined using DFT calculations and the calculated activation energies.

The group 6 metal fragments of the general type $Cp'ML_2$ (M = Cr, Mo, W; Cp′ = Cp, Cp*, Ind; L = 2e donors) have proven to be particularly able to stabilize ring-slipped cyclopentadienyl-like ligands coordinated in a trihapto (η^3-Cp′) fashion. The earliest example of a *de bona fide* bent (η^3-Cp) ligand structurally characterized, in CpW(η^3-Cp)$(CO)_2$,[1] the related η^3-Cp* in Cp*Cr(η^3-Cp*)$(CO)_2$,[2] and the first η^3-Ind ligand in IndW(η^3-Ind)$(CO)_2$[3] all confirm this fact. Our recent studies of a series of Ind(Cp′)ML_2 metallocenes (M = Mo, W; Cp′ = Cp, Ind)[4] produced several additional examples of η^3-Cp′ derivatives of the type Cp′M(η^3-Cp′)L_2 as well as deep insight into the factors that control $\eta^5 \rightarrow \eta^3$ haptotropic shift processes. One example concerns the fluorenyl derivative (η^5-Ind)Mo(η^3-Flu)$CO)_2$ (**1**) in which the fluorenyl ligand exhibits *exo*cyclic η^3-coordination.[5]

Theoretical calculations clearly demonstrated that this coordination mode was favored only on electronic grounds since no important steric constraints were revealed either in the crystal structure or in the calculations. Previous examples of this coordination mode pertained to very crowded molecules.[6,7] Following $2e^-$ chemical oxidation the cation [(η^5-Flu)-$IndMo(CO)_2]^{2+}$ is formed in which formal *endo*cyclic η^5-coordination of the fluorenyl ring is restored. These results are, therefore, relevant to the understanding of ring-slippage processes and are in accordance with studies of the PEt_3 catalyzed isomerization of (η^6-Flu)$Mn(CO)_3$ to (η^5-Flu)$Mn(CO)_3$ where the experimental evidence favored an *exo*cyclic η^3-Flu intermediate (or transition state) as that capable of providing the lowest activation energy.[8]

Previous ^{1}H NMR studies of IndMo(η^3-Flu)$(CO)_2$ (**1**) showed it to be fluxional at *ca.* 50 °C but no detailed study was carried out.[5] In the present paper we describe the synthesis of other IndMo(η^3-Flu′)$(CO)_2$ complexes with fluorenyl analogs, namely Flu′ = cyclopenta[*def*]phenanthrenyl and 8,9-dihydrocyclopenta[*def*]phenanthrenyl, and characterize their structures both in the solid state (X-ray) and in solution (NMR). DFT calculations provide a rationale for the *exo*cyclic coordination preference in these complexes.

Results and discussion

Synthetic aspects

Following a recently found reaction method,[9] IndMo(η^3-C_3H_5)$(CO)_2$ with HCl in CH_2Cl_2 gives an intermediate pink-red powder, which dissolves in toluene and reacts with LiFlu, Licpp and LiH_2cpp at low temperature to afford high yields of IndMo(η^3-Flu)$(CO)_2$ (**1**), (η^5-Ind)Mo(η^3-cpp)$(CO)_2$ (**2**) and (η^5-Ind)Mo(η^3-H_2cpp)$(CO)_2$ (**3**). These complexes **1**–**3** are more soluble in ether or hexane than other related complexes of the type Cp′Mo(η^3-Ind)L_2.[4] They are air and moisture sensitive and must be handled and stored under moisture-free inert gas atmosphere.

The KBr IR spectra of compounds **2** and **3** show the two typical ν(CO) stretching vibration bands in the range 1940–1854 cm^{-1}, similar to those previously reported for **1**.[5]

 DOI: 10.1039/b204418h

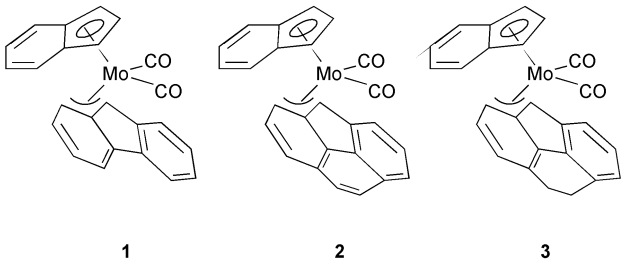

Solution NMR

The ^{1}H 1D NMR spectra for all three complexes are consistent with the proposed structures with η^3-Flu coordination (see Experimental for numbering). The aromatic protons of all the complexes appear in the region 8–7 ppm. The H3 proton of the Flu, cpp and H_2cpp ligands appears around 2.5 ppm with the H5 proton at around 4 ppm. The rest of the protons of the Flu type ligands appear in the 7–8 ppm region. The H24–H27 protons of the Ind unit appear in the 7–8 ppm region while the H21 protons appear at *ca.* 5.5 ppm and the H22 and H23 protons in the region 6–6.5 ppm. For all three complexes the lines appear sharp with no indication of exchange. However, a 2D NOESY spectrum of Mo-Flu (**1**) (600 ms mix) indicated the presence of exchange cross peaks (the same sign as the diagonal and the opposite sign from the NOESY cross peaks) between the H5 and H14, H6 and H13 and the H7 and H12 protons of the Flu ligand. There was also an exchange cross peak between the H21 and H23 protons of the Ind ligand. This is consistent with slow exchange (even at 303 K) of the Ind$Mo(CO)_2$ fragment between the pseudo-allylic positions defined by C14–C15–C3 and C3–C4–C5 (ring slippage, see below for numbering scheme). This type of fluxionality was not observed in the more rigid ansa-bridged complexes [{$Me_2C(\eta^5$-$C_5H_4)(\eta^3$-$C_{13}H_8)$}$Zr(\eta^5$-$C_5H_5)Cl$] and $[Me_2C(C_5H_4)(Flu)Zr(\mu$-$H)Cl]_2$.[6,7]

By increasing the temperature and recording 1D NMR spectra it was possible to compare the behavior of the 3 complexes. Fig. 1 shows the H5 proton of the Flu type ligand in the 3 complexes as the temperature is raised from 303 to 318 K. It can be seen that for Mo-Flu (**1**) and Mo-H_2cpp (**3**) the lines broaden considerably as the temperature is raised while Mo-cpp shows much less broadening. Measurements at temperatures greater than 318 K could not be carried out due to the solvent used in the NMR experiments. By observing the linewidths of the NMR resonances the order of ease of ring slippage can be estimated: Mo-H_2cpp > Mo-Flu > Mo-cpp.

The unusual *exo*cyclic coordination mode for complexes **1**–**3** is therefore confirmed by these data. In contrast to the two other known *exo*cyclic compounds,[6,7] neither ansa-bridging nor important steric crowding force the observed *exo*cyclic bonding.

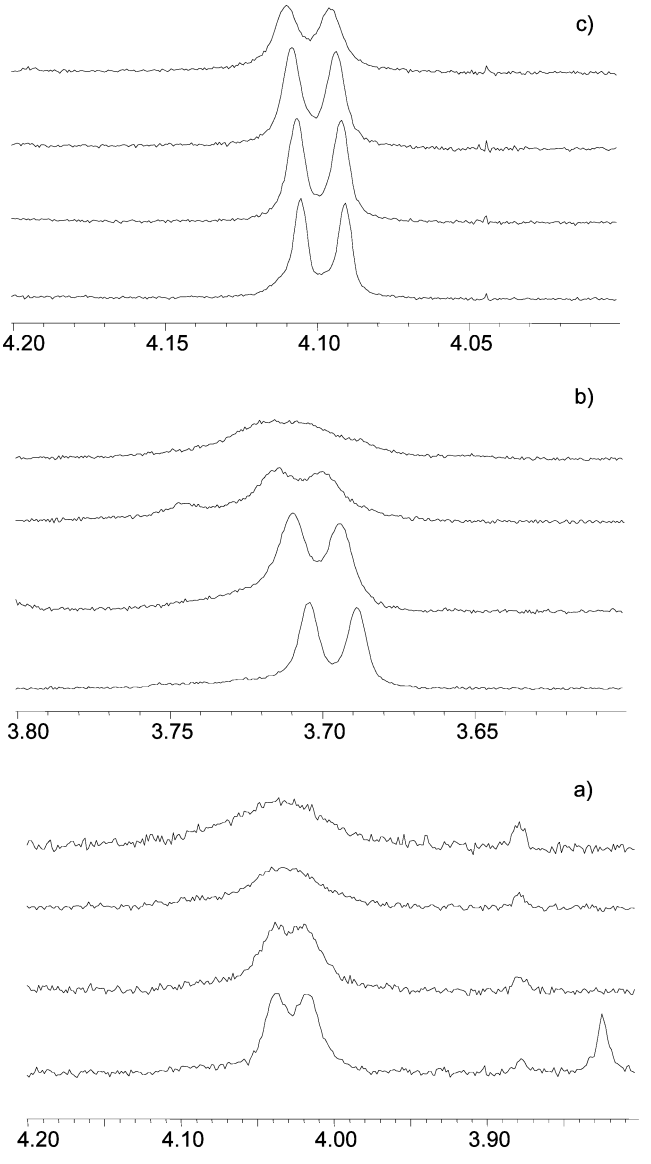

Fig. 1 Variable temperature ^{1}H NMR spectra of the H5 proton in (a) (η^5-Ind)Mo(η^3-H_2cpp)$(CO)_2$ (**3**), (b) (η^5-Ind)Mo(η^3-Flu)$(CO)_2$ (**1**), and (c) (η^5-Ind)Mo(η^3-cpp)$(CO)_2$ (**2**). Spectra are shown at 303 (bottom), 308, 313 and 318 K (top).

Crystallography

The crystal structures of compounds (η^5-Ind)$Mo(CO)_2(\eta^3$-ccp) (**2**) and (η^5-Ind)$Mo(CO)_2(\eta^3$-H_2ccp) (**3**) were determined using single-crystal X-ray diffraction analysis. The molecular structures in the solid state of both complexes are identical within the standard limits (except for atoms C16 and C17) and very similar to the molecular structure of compound **1**.[5] Therefore the present discussion of complex **2** will also be valid for complexes **1** and **3**. An ORTEP style plot with the appropriate numbering scheme is shown in Fig. 2. Selected bond distances and angles are listed in Table 1.

The crystal structure consists of discrete (η^5-Ind)-$Mo(CO)_2(\eta^3$-ccp) molecules in the unit cell. No significant short inter- and/or intramolecular contacts are observed. Only the hydrogens attached to the metal-coordinated carbon atoms C3 and C5 are located out of the plane of the cyclopentaphenantrenyl moiety (Fig. 3).

The molybdenum atom is bonded to two carbonyl groups, one η^5-indenyl ligand and one η^3-cyclopentaphenantrenyl ligand (*exo*cyclic, π-allylic), which adopts an *endo* confirmation with respect to the (η^5-Ind)$Mo(CO)_2$ fragment. This distorted tetrahedral geometry at the central metal atom is identical, within small deviations, to all other structurally characterized complexes of the type [(η^5-Ind)$Mo(CO)_2$-{η^3-(π-allyl)}].[10] The range of the distances observed for the five Mo–C bonds, 2.306(2)–2.449(2) Å [**1**: 2.302(2)–2.456(2) Å; **3**: 2.286(2)–2.476(2) Å], the slip-parameter Δ value of 0.16 Å [**1**: 0.18 Å; **3**: 0.21 Å], and the fold angle Ω of 5.51° [**1**: 5.45°; **3**: 5.62°] are consistent with typical $\eta^3+\eta^2$ indenyl coordination (see ref. 4*a* for definitions and values of Δ and Ω for similar systems). Distances and angles within the organic ligands are unexceptional and do not require further comment. NMR and IR data are in excellent agreement with these observations.

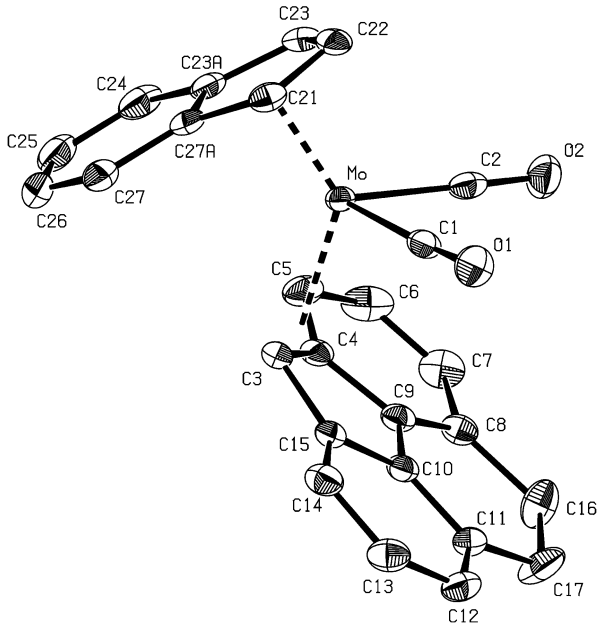

Fig. 2 ORTEP[21e] representation of compound **3** in the solid state. Thermal ellipsoids are at the 50% probability level. Hydrogen atoms omitted for clarity. Compounds **1** and **2** have the same numbering system and identical overall geometry (see Table 1).

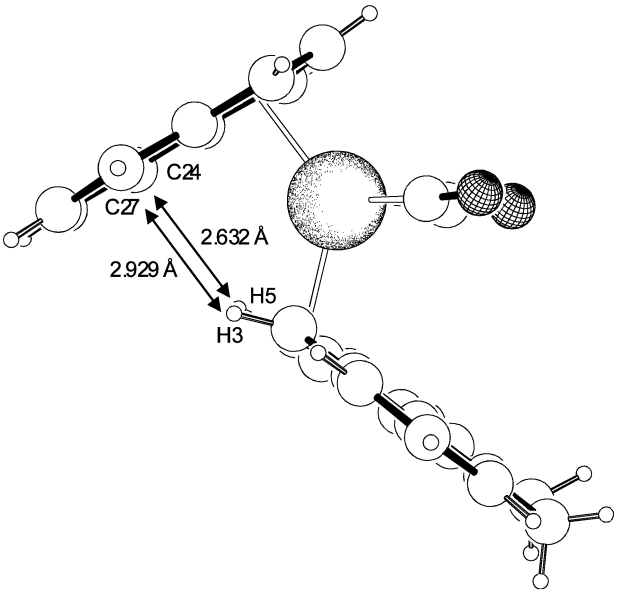

Fig. 3 PLATON[21e] schematic view of compound **3** showing the *out of plane* disposition of H3 and H5.

Theoretical study

Previous work[5] has shown, by means of DFT calculations[11] (ADF program),[12] that the η^3-fluorenyl anion exhibits a preference for *exo* coordination, contrary to what is observed with η^3-indenyl. Another difference between the two ring systems is that coordination of three carbon atoms of the central ring of a fluorenyl ligand, either *endo* or *exo*, cannot be accompanied by folding, owing to the rigidity of the three fused rings. The indenyl ligand, however, usually folds.[13,14]

The great tendency of indenyl to undergo ring slippage from η^5- to η^3-indenyl, when compared to cyclopentadienyl, has been traditionally explained by the aromaticity of the remaining non-coordinated benzene.[15] This interpretation has been recently challenged.[4c]

Coordination possibilities and the competition for electrons between rings can be used as another independent way of testing this idea. Fluorenyl is a 14-electron system that will leave behind a 10-electron fragment when η^3-coordinated. Fusing an extra ring, as in the cpp anion, adds two more π electrons, thus destroying aromaticity. The H_2cpp ligand is identical to fluorenyl from this point of view. It has been demonstrated above that the molecular structures of the three complexes discussed in this work are very similar; the indenyl ring always remains η^5, while the larger ring undergoes slippage, becoming η^3-coordinated. The differences in behavior between complexes carrying different rings can be probed using NMR and should reflect the binding energy of each ring to the (Ind)Mo(CO)$_2$ fragment.

DFT calculations (Gaussian98[16] and ADF; see Experimental for details) were performed on these three compounds in order to obtain bond strength indicators. The first step consisted of a full geometry optimization. As the fluorenyl complex has been discussed before,[5] (η^5-Ind)Mo(η^3-cpp)(CO)$_2$ (**2**) will be analyzed in more detail here. Both DFT programs led to a very good agreement between the experimental and calculated structures, as can be seen in Fig. 4.

The differences in bond lengths are very small for the B3LYP and even smaller for the ADF calculations, probably due to the better quality of the basis set. The Mo–C distances involving the C_5 ring of indenyl exhibit the 3 shorter plus 2 longer distribution typical of the $\eta^3 + \eta^2$ coordination mode of this ligand. The cpp ring shows one longer and two shorter Mo–C bonds, all the other distances being above 3 Å, well outside bonding range. It is interesting to note that the two hydrogen atoms bound to the coordinated carbon atoms of the cpp also appear out of the cpp plane in the calculations, emphasizing the fact that electronic effects are behind this behavior. This is a well known feature of coordinated rings[17] and is not observed more frequently owing to the difficulty in accurately locating hydrogen atoms by X-ray diffraction methods. This distortion redirects the carbon orbitals so that there is better metal-carbon overlap and therefore stronger bonding.

Taking into account the fact that the calculations seem to be reliable and the complexes are adequately described, the strength of the bond between the large rings and the (η^5-Ind)Mo(CO)$_2$ fragment was studied.

Table 1 Selected interatomic distances (Å) and angles (deg) for compounds **1**, **2** and **3**

	1[5]	**2**	**3**
Mo–C1	1.946(2)	1.940(2)	1.941(2)
Mo–C2	1.964(2)	1.943(2)	1.951(2)
Mo–C3	2.334(2)	2.349(2)	2.334(2)
Mo–C4	2.368(2)	2.359(2)	2.372(2)
Mo–C5	2.497(2)	2.517(2)	2.537(2)
Mo–C21	2.302(2)	2.314(2)	2.295(2)
Mo–C22	2.303(2)	2.306(2)	2.286(2)
Mo–C23	2.335(3)	2.318(3)	2.330(3)
Mo–C23A	2.456(2)	2.443(2)	2.476(2)
Mo–C27A	2.444(2)	2.449(2)	2.447(2)
C1–O1	1.152(3)	1.156(3)	1.159(3)
C2–O2	1.150(3)	1.153(3)	1.154(3)
C21–C22	1.418(4)	1.411(3)	1.415(3)
C21–C27A	1.441(3)	1.438(3)	1.433(3)
C22–C23	1.418(4)	1.407(3)	1.409(3)
C23–C23A	1.438(3)	1.436(3)	1.439(3)
C23A–C27A	1.429(3)	1.437(3)	1.435(3)
C1–Mo–C2	77.85(8)	76.96(8)	79.71(8)
Mo–C1–O1	176.8(2)	177.4(2)	176.6(2)
Mo–C2–O2	177.9(2)	177.7(2)	178.5(2)
C3–C4–C5	129.0(2)	134.1(2)	133.8(2)
C3–C15–C14	130.5(2)	137.3(2)	136.0(2)
Ind–Mo–Flu/cpp/H_2cpp	129.0	130.5	129.3

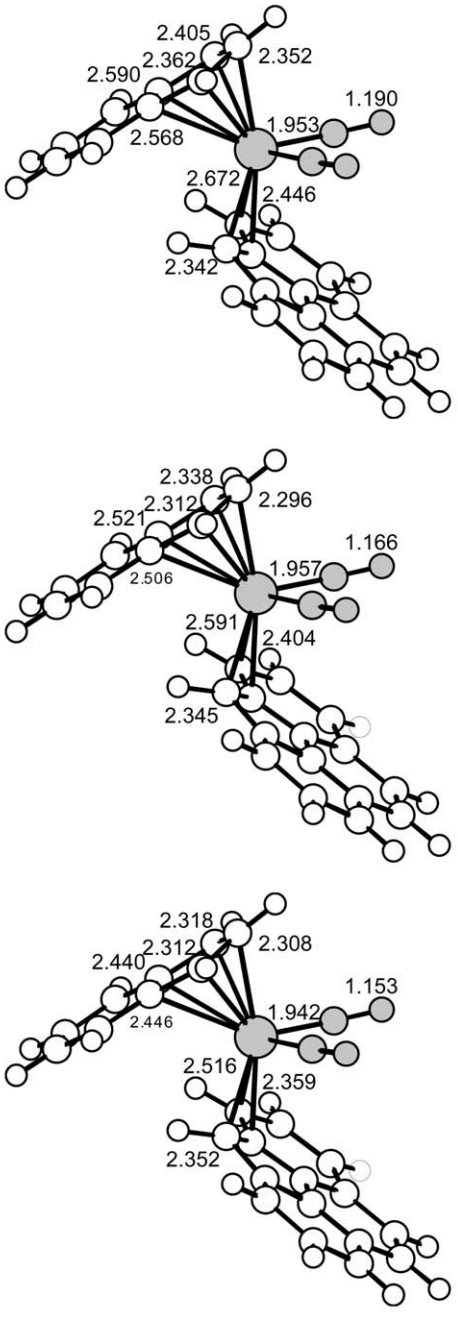

Fig. 4 Some relevant distances in the structure of (η^5-Ind)Mo(η^3-cpp)$(CO)_2$ (**2**): calculated (DFT/B3LYP, top; DFT/ADF, center) and experimental (bottom). The $Mo(CO)_2$ fragment is shaded, for clarity.

One way of obtaining good indicators for the metal-ring bond strength is *via* Wiberg indices and has been used before, with success, in bond strength estimation in $Mo(Cp')_2(CO)_2$ ($Cp' = Cp$, Ind) systems.[4c] The sum of calculated Mo–C Wiberg indices for the three coordinated C atoms of each ring amounts to 0.811 for fluorenyl, 0.816 for cpp, and 0.798 for H_2cpp, indicating a stronger bond in the case of cpp, in accordance with less fluxionality. Extended Hückel calculations using fixed Mo–C distances led to a higher overlap population, a measure of bond strength, between the anionic ring and the cationic metal fragment for cpp (0.12) than for fluorenyl and H_2cpp (0.11), again reflecting a stronger bond in the case of cpp. This result was previously discussed in detail for the $[(\eta^3\text{-X})Mn(CO)_3]^{2-}$ system,[13] where a less crowded metal coordination sphere allows a linear relationship between the

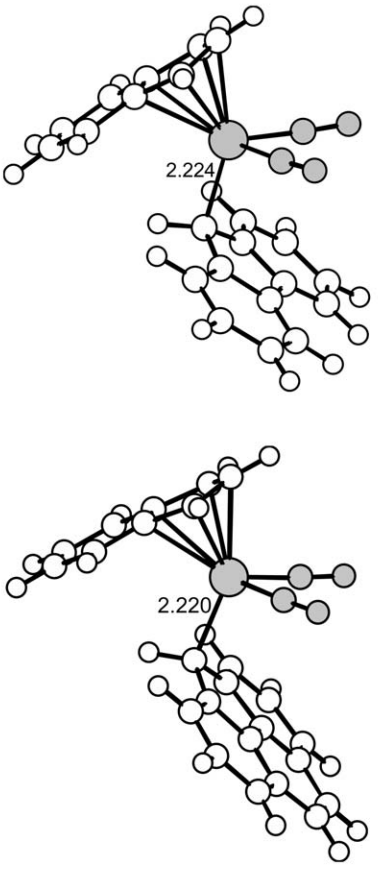

Fig. 5 The transition states for the migration of molybdenum from one side of the ring to the other in (η^5-Ind)Mo(η^3-X)$(CO)_2$, for X = Flu (top) and X = cpp (bottom), with indication of the Mo–C distance. The $Mo(CO)_2$ fragment is shaded, for clarity.

M–(η^3-X) bond strength and the geometrical parameters, namely shorter M–C(X) bond lengths for X = cpp than for X = Flu.

A bonding energy decomposition scheme performed with ADF[18] indicated that they were very similar (within 1.5 kcal mol^{-1}) for the three complexes.

Since it is difficult to explain the reactivity of the complexes solely from ground state effects, transition states for the migration of the metal from one side of the ring (η^3-X) to the other side (also η^3-X) were searched for with X = Flu and cpp only (since H_2cpp behaves as fluorenyl). In each case the transition state corresponds to the η^1-coordination mode of the ring, as shown in Fig. 5.

The calculated activation barriers are 14.4 and 14.7 kcal mol^{-1}, respectively, for fluorenyl and cpp, reflecting the observed fluxionality of cpp at higher temperatures. In the transition state, the M–C bond is stronger for cpp, as reflected both in the Wiberg index (0.559, compared to 0.544 for fluorenyl) and distance (2.220 Å, compared to 2.224 Å for fluorenyl).

Conclusions

As shown by X-ray crystallography studies, the coordination of the fluorenyl ring (Flu) and its related analogs cyclopenta[*def*]phenanthrenyl (cpp) and 8,9-dihydrocyclopenta[*def*]phenanthrenyl (H_2cpp) to the 15-electron fragment (η^5-Ind)-$Mo(CO)_2$, [Mo], takes place in an η^3-exocyclic fashion. No intramolecular steric repulsions were identified as possible causes for this preference and, therefore, this coordination mode is dictated by electronic effects. Fluxional exchange of

the metal fragment over the two pseudo allylic positions on both sides of the bridgehead C–H fragment of the C_5 ring in the fluorenyl type ligands was observed. This exchange process ensues at lower temperatures for [Mo]-H_2cpp and [Mo]-Flu than for [Mo]-cpp. DFT calculations are found to be in accord with both the electronic preference for η^3-exocyclic coordination of the fluorenyl type rings and the order of energies for the exchange process. The cpp ligand makes a stronger bond to the [Mo] fragment than the other two congeners. The calculated transition state for these exchange processes involves a [Mo]–(η^1-Flu) coordination.

Experimental

All operations were carried out under an atmosphere of dinitrogen with standard Schlenk line and glovebox techniques. Solvents were purified by conventional methods and distilled under nitrogen prior to use. NMR spectra in acetone-d_6 were measured on Bruker CXP 300, ARX 400 and DMX 600 spectrometers. IR spectra were measured on a Unicam Mattson model 7000 FTIR spectrometer. IndMo(η^3-C_3H_5)$(CO)_2$[4,19] and LiFlu[20] were prepared following published procedures.

Syntheses

Preparation of Licpp and LiH_2cpp. The compounds were prepared following the method published for LiFlu.[20] A solution of cppH (0.3 g; 1.57 mmol) in hexane was cooled to −30 °C and *n*-butyl lithium (1 mL of a 1.6 M hexane solution, 1.57 mmol) was added. The reaction mixture was stirred at −30 °C for 1 h and then allowed to warm to room temperature. After a further 16 h of stirring a pale yellow precipitate was isolated by filtration, washed with hexane and dried under vacuum. The yield of Licpp was quantitative (0.30 g).

LiH_2cpp was similarly prepared from H_2cppH (0.3 g, 1.56 mmol) and *n*-BuLi (1 mL, 1.56 mmol), also in quantitative yield.

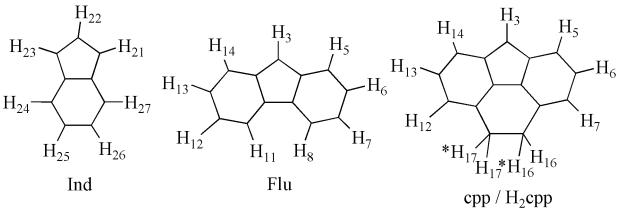

Preparation of (η^5-Ind)Mo(η^3-Flu)$(CO)_2$ (1). Gaseous HCl was bubbled through a solution of IndMo(η^3-C_3H_5)$(CO)_2$ (1.07 g, 2.67 mmol) in CH_2Cl_2 (30 mL) for 3 min and the mixture was stirred for a further 10 h to complete the reaction. The dark red solution was evaporated, washed with hexane, and dried under vacuum. A mixture of LiFlu (0.46 g, 2.67 mmol) and the resulting residue was placed in a cold bath at −30 °C. Precooled toluene was added and the temperature was slowly raised to room temperature. After 16 h, the solution was filtered through celite and the filtrate was concentrated to dryness to give a red crystalline solid. Recrystallization of **1** in a toluene–hexane mixture afforded red crystals suitable for an X-ray diffraction study. Yield: (1.04 g, 90%). Found: C, 66.49; H, 3.68. $C_{24}H_{16}O_2Mo$ (432.33) requires: C, 66.67; H 3.70%. IR(KBr) selected ν_{max}/cm^{-1}: 1942 and 1853, *vs.* ν(CO). δ_H (400 MHz, acetone-d_6, 303 K, $SiMe_4$): 7.8–7.0 (m, 11H, H14–H11, H24–H27, H6–H8), 6.44 (s, 1H, H21), 6.26 (s, 1H, H23), 5.30 (t, 1H, H22), 3.70 (d, 1H, H5), 2.45 (s, 1H, H3).

Preparation of (η^5-Ind)Mo(η^3-cpp)$(CO)_2$ (2). Gaseous HCl was bubbled through a solution of IndMo(η^3-C_3H_5)$(CO)_2$ (0.63 g, 1.57 mmol) in CH_2Cl_2 (25 mL) for 3 min and the mixture was stirred for a further 10 h to complete the reaction. The dark red solution was evaporated, washed with hexane, and dried under vacuum. A mixture of Licpp (0.30 g, 1.57 mmol) and the resulting residue in toluene was placed in a cold bath at −20 °C. The reaction mixture was stirred for 1 h at low temperature and then allowed to warm up to room temperature and stirred for a further 12 h. The solution was filtered through celite and the filtrate concentrated to dryness to give a red crystalline solid. Recrystallization of **2** in a toluene–hexane mixture gave red crystals suitable for an X-ray diffraction study. Yield: (0.63 g, 88%). Found: C, 68.40; H, 3.58. $C_{26}H_{16}O_2Mo$ (456.36) requires: C, 68.43; H, 3.53%. IR(KBr) selected ν_{max}/cm^{-1}: 1941 and 1854 *vs.* ν(CO). δ_H (400 MHz, acetone-d_6, 303 K, $SiMe_4$): 8.1–7.3 (m, 11H, H14–H17, H24–H27, H6–H16), 6.46 (s, 1H, H21), 6.27 (s, 1H, H23), 5.33 (t, 1H, H22), 4.10 (d, 1H, H5), 3.04 (s, 1H, H3).

Preparation of (η^5-Ind)Mo(η^3-H_2cpp)$(CO)_2$ (3). Gaseous HCl was bubbled through a solution of IndMo(η^3-C_3H_5)$(CO)_2$ (0.83 g, 2.06 mmol) in CH_2Cl_2 (25 mL) for 3 min and the mixture was stirred for a further 10 h to complete the reaction. The dark red solution was evaporated, washed with hexane, and dried under vacuum. A mixture of LiH_2cpp (0.41 g, 2.06 mmol) and the resulting residue was placed in a cold bath at −30 °C. Precooled toluene was added and the temperature was slowly raised to room temperature and the solution stirred for a further 8 h. The solution was filtered through celite and the filtrate concentrated to dryness to give a red crystalline solid. Recrystallization of **3** in a toluene–hexane mixture gave red crystals suitable for an X-ray diffraction study. Yield: (0.80 g, 85%. Found: C, 68.21; H, 3.97. $C_{26}H_{18}O_2Mo$ (458.37) requires: C, 68.13; H, 3.96%. IR(KBr) selected ν_{max}/cm^{-1}: 1940 and 1855 *vs.* ν(CO). δ_H (400 MHz, acetone-d_6, 303 K, $SiMe_4$): 7.70–6.80 (m, 9H, H12–H14, H24–H27, H6–H7), 6.44 (s, 1H, H21), 6.20 (s, 1H, H23), 5.30 (t, 1H, H22), 4.03 (d, 1H, H5), 3.08 (s, 2H, H2 unit), 3.07 (s, 2H, H2 unit), 2.64 (s, 1H, H3).

X-Ray structure determination of complexes 2 and 3

Details of the X-ray experiment, data reduction, and final structure refinement calculation are summarized in Table 2. Crystals suitable for X-ray structure determinations were grown in a saturated solution of complexes **2** and **3** in a toluene–hexane mixture. Preliminary examination and data collection were carried out on an image plate diffraction system (IPDS; Stoe & Cie) equipped with a rotating anode [Nonius FR591; 50 (50) kV; 80 (60) mA; 4.0 (3.0) kW] and graphite monochromated MoK_α radiation (λ = 0.71073 Å). Data collection was performed at 123 (173) K with an exposure time of 120 (150) s per image [phi scans, rotation modus from $\varphi = 0°$ to 360°, $\Delta\varphi = 1.5°$ (2.0°)]. A total of 25644 (12871) reflections were collected. After merging 3481 (3291) independent reflections remained and were used for all calculations. Data were corrected for Lorentz and polarization effects.[21a] Corrections for absorption and decay effects were not applied. The unit cell parameters were obtained by full-matrix least-squares refinements of 4934 (4881) reflections with the program CELL.[21a] The structure was solved by a combination of direct methods and difference-Fourier syntheses.[21b] All non-hydrogen atoms of the asymmetric unit were refined with anisotropic thermal displacement parameters. All hydrogen atoms were found in the difference Fourier map and refined freely with individual isotropic thermal displacement parameters. Full-matrix least-squares refinements were carried out by minimizing $\Sigma w(F_o^2 - F_c^2)^2$ with a SHELXL-97 weighting scheme and stopped at a maximum shift/err < 0.001.[21c] Neutral atom scattering factors for all atoms and anomalous dispersion corrections for the non-hydrogen atoms were taken from the

Table 2 Crystal data and structure refinement of complexes **2** and **3**

	2	**3**
Formula	$C_{26}H_{16}MoO_2$	$C_{26}H_{18}MoO_2$
FW	456.33	458.37
Crystal system	Monoclinic	Triclinic
Space group	$P\,2_1/n$ (No. 14)	$P\bar{1}$ (No. 2)
a/Å	9.7600(8)	9.1945(11)
b/Å	10.8026(10)	9.7882(11)
c/Å	17.744(2)	10.9604(12)
α/deg	90	91.929(14)
β/deg	95.899(10)	106.072(13)
γ/deg	90	99.804(15)
U/Å^3	1860.9(3)	930.6(2)
Z	4	2
T/K	123	173
μ/mm^{-1}	0.725	0.725
Collect. reflect.	25 644	12 871
Indep. reflect.	3481	3291
R_{int}	0.0295	0.0329
Obsd. reflect. [$I > 2\sigma(I)$]	3175	2956
R_1 (obsd)	0.0222	0.0205
R_1(all)	0.0249	0.0244
wR_2 (obsd)	0.0587	0.0515
wR_2 (all)	0.0598	0.0523

International Tables for Crystallography.[21d] All other calculations (including ORTEP graphics) were done with the program PLATON.[21e] Calculations were performed on a PC workstation (Intel Pentium II) running LINUX.

CCDC reference numbers 189190 for **2** and 189189 for **3**. See http://www.rsc.org/suppdata/nj/b2/b204418h/ for crystallographic data in CIF or other electronic format.

Computational details

The calculations were performed by means of *ab initio* and DFT methods within the Gaussian 98 program.[16] The B3LYP hybrid functional was used in all calculations. This functional includes a mixture of Hartree–Fock[22] exchange with DFT[11] exchange-correlation, given by Becke's three-parameter functional[23] with the Lee, Yang and Parr correlation functional, which includes both local and non-local terms.[24,25] Full geometry optimizations were carried out without any symmetry constraints, using a standard LanL2DZ[26,27] basis set. A natural bond orbital analysis (NBO)[28] was performed and the evaluated Wiberg indexes[29] used as a measure of the flu′–M (Flu′ = Flu, cpp, H_2cpp) bond strength. Transition state optimizations were performed with the synchronous transit-guided quasi-Newton method (STQN) developed by Schlegel *et al.*[30] The transition state determinations were confirmed by frequency calculations yielding one imaginary frequency, and by visual analysis of this frequency. Single-point energy calculations were performed on the optimized geometries at the same theory level, with a standard 6-31G** basis set[31] for C, H and O, and a standard 3-21G basis set[32] with an added f polarization function[33] for Mo.

Density functional calculations[11] were carried out with the Amsterdam density functional (ADF2000) program developed by Baerends and coworkers.[12] Vosko, Wilk and Nusair's local exchange correlation potential was used.[34] Gradient corrected geometry optimizations[35] were performed using the generalized gradient approximation (Becke's exchange[36] and Perdew's[37] correlation functionals), and included relativistic effects, treated by the ZORA formalism.[38]

An uncontracted triple-ζ nd, $(n+1)$s STO basis set was used for Mo, augmented by one $(n+1)$p function and a single-ζ polarization function. The valence shells for C, N, O (2s,2p), and P, S (3s,3p) were described by an uncontracted triple-ζ STO basis set, augmented by two polarization functions: 3d and 4f. For H an uncontracted triple-ζ STO basis set (1s) with two polarization functions, 2p and 3d, was used. The inner shells of Mo ([1–4]s,[2–4]p, 3d), C (1s), O (1s), P (1s, 2s, 2p) and S (1s, 2s, 2p) were frozen. The full geometry optimizations were performed without any symmetry constraints.

Extended Hückel calculations. The extended Hückel calculations[39] were done with the CACAO program[40] and modified H_{ij} values were used.[41] The basis set for the metal atoms consisted of ns, np and $(n-1)$d orbitals. The s and p orbitals were described by single Slater-type wave functions, and the d orbitals were taken as contracted linear combinations of two Slater-type wave functions. The parameters used for Mo were the following (H_{ii} eV, ζ): 5s − 8.77, 1.960; 5p − 5.60, 1.900; 4d − 11.06, 4.542 (ζ_1), 1.901 (ζ_2), 0.5899 (C_1), 0.5899 (C_2). Standard parameters were used for other atoms. Calculations were performed on models based on the optimized geometries with idealized maximum symmetry.

Acknowledgements

This work was partially financed by PRAXIS XXI under Projects PRAXIS XX1.2/2.1/QUI/316/94, PBIC/QUI/2201/95 and POCTI/36127/QUI/2000. BR thanks PRAXIS XXI for a post-doctoral grant. EH thanks Dr. S. Tiling-Grosse for her support in completing our X-ray instrumentation. BJG would like to thank Dr. Victor Wray at the Gesellschaft für Biotecnologische Forschung (GBF-Braunschweig, Germany) for use of the DMX600 NMR spectrometer.

References

1 G. Huttner, H. H. Brintzinger, L. G. Bell, P. Friedrich, V. Bejenke and D. Neugebauer, *J. Organomet. Chem.*, 1978, **145**, 329.
2 E. U. van Raaij, H. H. Brintzinger, L. Zsolnai and G. Huttner, *Z. Anorg. Allg. Chem.*, 1989, **577**, 217.
3 A. N. Nesmeyanov, N. A. Ustynyuk, L. G. Makarova, V. G. Andrianov, Y. T. Struchkov, S. J. Andrae, Y. A. Ustynyuk and S. G. Malyugina, *J. Organomet. Chem.*, 1978, **159**, 189.
4 (*a*) J. R. Ascenso, C. G. Azevedo, I. S. Gonçalves, E. Herdtweck, D. S. Moreno, C. C. Romão and J. Zühlke, *Organometallics*, 1994, **13**, 429; (*b*) M. J. Calhorda, C. A. Gamelas, I. S. Gonçalves, E. Herdtweck, C. C. Romão and L. F. Veiros, *Organometallics*, 1998, **17**, 2597; (*c*) M. J. Calhorda, C. C. Romão and L. F. Veiros, *Chem. Eur. J.*, 2002, **8**, 868.
5 M. J. Calhorda, I. S. Gonçalves, E. Herdtweck, C. C. Romão, B. Royo and L. F. Veiros, *Organometallics*, 1999, **18**, 3956.
6 G. M. Diamond, M. L. H. Green, P. Mountford, N. A. Popham and A. N. Chernega, *J. Chem. Soc., Chem. Commun.*, 1994, 103.
7 M. Bochmann, S. J. Lancaster, M. B. Hursthouse and M. Mazid, *Organometallics*, 1993, **12**, 4718.
8 (*a*) R. N. Biagioni, I. M. Lorkovic, J. Skelton and J. B. Hartung, *Organometallics*, 1990, **9**, 547; (*b*) M. E. Rerek and F. Basolo, *Organometallics*, 1984, **3**, 647.
9 M. G. B. Drew, V. Félix, I. S. Gonçalves, C. C. Romão and B. Royo, *Organometallics*, 1998, **17**, 5782.
10 3d Search and research using the Cambridge Structural Database, F. H. Allen and O. Kennard, *Chem. Des. Auto. News*, 1993, **8**, 1; F. H. Allen and O. Kennard, *Chem. Des. Auto. News*, 1993, **8**, 31–37. The refcodes are: BAMGUR, CETYUV, DAMBIC, FAWMOF, NEZWAO, PEWMOT, PEWMUZ, VEBLET, YUMSUU, YUMSUU10, and ZEGTUA.
11 R. G. Parr and W. Yang, *Density Functional Theory of Atoms and Molecules*, Oxford University Press, New York, 1989.
12 (*a*) E. J. Baerends, A. Bérces, C. Bo, P. M. Boerrigter, L. Cavallo, L. Deng, R. M. Dickson, D. E. Ellis, L. Fan, T. H. Fischer, C. Fonseca Guerra, S. J. A. van Gisbergen, J. A. Groeneveld, O. V. Gritsenko, F. E. Harris, P. van den Hoek, H. Jacobsen, G. van Kessel, F. Kootstra, E. van Lenthe, V. P. Osinga, P. H. T. Philipsen, D. Post, C. C. Pye, W. Ravenek, P. Ros, P. R. T. Schipper, G. Schreckenbach, J. G. Snijders, M. Sola, D. Swerhone, G. te Velde, P. Vernooijs, L. Versluis, O. Visser,

E. van Wezenbeek, G. Wiesenekker, S. K. Wolff, T. K. Woo, and T. Ziegler, ADF, Amsterdam, 1999; (*b*) C. Fonseca Guerra, O. Visser, J. G. Snijders, G. te Velde and E. J. Baerends, in *Methods and Techniques for Computational Chemistry*, eds., E. Clementi and C. Corongiu, STEF, Cagliari, 1995, p. 303–395; (*c*) C. Fonseca Guerra, J. G. Snijders, G. te Velde and E. J. Baerends, *Theor. Chem. Acc.*, 1998, **99**, 391; (*d*) E. J. Baerends, D. Ellis and P. Ros, *Chem. Phys.*, 1973, **2**, 41; (*e*) E. J. Baerends and P. Ros, *Int. J. Quantum Chem.*, 1978, **S12**, 169; (*f*) P. M. Boerrigter, G. te Velde and E. J. Baerends, *Int. J. Quantum Chem.*, 1988, **33**, 87; (*g*) G. te Velde and E. J Baerends, *J. Comput. Phys.*, 1992, **99**, 84.
13 L. F. Veiros, *J. Organomet. Chem.*, 1999, **587**, 221.
14 M. J. Calhorda and L. F. Veiros, *Comments Inorg. Chem.*, 2001, **22**, 375.
15 A. J. Hart-Davis and R. J. Mawby, *J. Chem. Soc. A*, 1969, 2403.
16 M. J. Frisch, G. W. Trucks, H. B. Schlegel, G. E. Scuseria, M. A. Robb, J. R. Cheeseman, V. G. Zakrzewski, Jr., J. A. Montgomery, R. E. Stratmann, J. C. Burant, S. Dapprich, J. M. Millam, A. D. Daniels, K. N. Kudin, M. C. Strain, O. Farkas, J. Tomasi, V. Barone, M. Cossi, R. Cammi, B. Mennucci, C. Pomelli, C. Adamo, S. Clifford, J. Ochterski, G. A. Petersson, P. Y. Ayala, Q. Cui, K. Morokuma, D. K. Malick, A. D. Rabuck, K. Raghavachari, J. B. Foresman, J. Cioslowski, J. V. Ortiz, A. G. Baboul, B. B. Stefanov, G. Liu, A. Liashenko, P. Piskorz, I. Komaromi, R. Gomperts, R. L. Martin, D. J. Fox, T. Keith, M. A. Al-Laham, C. Y. Peng, A. Nanayakkara, C. Gonzalez, M. Challacombe, P. M. W. Gill, B. Johnson, W. Chen, M. W. Wong, J. L. Andres, C. Gonzalez, M. Head-Gordon, E. S. Replogle and J. A. Pople, Gaussian 98, rev. A.7, Gaussian, Inc., Pittsburgh PA, 1998.
17 M. Elian, M. M. L. Chien, D. M. P. Mingos and R. Hoffmann, *Inorg. Chem.*, 1976, **15**, 1148.
18 (*a*) T. Ziegler and A. Rauk, *Inorg. Chem.*, 1979, **18**, 1755; (*b*) T. Ziegler and A. Rauk, *Inorg. Chem.*, 1979, **18**, 1758; (*c*) T. Ziegler and A. Rauk, *Theor. Chim. Acta*, 1977, **46**, 1.
19 J. R. Ascenso, I. S. Gonçalves, E. Herdtweck and C. C. Romão, *J. Organomet. Chem.*, 1996, **508**, 169.
20 J. Okuda, F. J. Schattenmann, S. Wocadlo and W. Massa, *Organometallics*, 1995, **14**, 789.
21 (*a*) IPDS Operating System, v. 2.8, Stoe & Cie. GmbH, Darmstadt, Germany, 1997; (*b*) SIR92: A. Altomare, G. Cascarano, C. Giacovazzo, A. Guagliardi, M. C. Burla, G. Polidori and M. Camalli, *J. Appl. Crystallogr.*, 1994, **27**, 435; (*c*) G. M. Sheldrick, SHELXL-97, University of Göttingen, Göttingen, Germany, 1998; (*d*) *International Tables for Crystallography*, ed. A. J. C. Wilson, Kluwer Academic Publishers, Dordrecht, The Netherlands, 1992, vol. C, tables 6.1.1.4 (pp. 500–502), 4.2.6.8 (pp. 219–222), and 4.2.4.2 (pp. 193–199); (*e*) A. L. Spek, PLATON, A Multipurpose Crystallographic Tool, Utrecht University, Utrecht, The Netherlands, 1999..
22 W. J. Hehre, L. Radom, P. R. Schleyer and J. A. Pople, *Ab Initio Molecular Orbital Theory*, John Wiley & Sons, New York, 1986.
23 A. D. Becke, *J. Chem. Phys.*, 1993, **98**, 5648.
24 C. Lee, W. Yang and R. G. Parr, *Phys. Rev. B*, 1988, **37**, 785.
25 B. Miehlich, A. Savin, H. Stoll and H. Preuss, *Chem. Phys. Lett.*, 1989, **157**, 200.
26 T. H. Dunning, Jr. and P. J. Hay, *Modern Theoretical Chemistry*, ed. H. F. Schaefer III, Plenum, New York, 1976, vol. 3, p. 1.
27 (*a*) P. J. Hay and W. R. Wadt, *J. Chem. Phys.*, 1985, **82**, 270; (*b*) W. R. Wadt and P. J. Hay, *J. Chem. Phys.*, 1985, **82**, 284; (*c*) P. J. Hay and W. R. Wadt, *J. Chem. Phys.*, 1985, **82**, 2299.
28 (*a*) J. E. Carpenter and F. Weinhold, *J. Mol. Struct. (Theochem)*, 1988, **169**, 41; (*b*) J. E. Carpenter, PhD Thesis, University of Wisconsin, Madison WI, 1987; (*c*) J. P. Foster and F. Weinhold, *J. Am. Chem. Soc.*, 1980, **102**, 7211; (*d*) A. E. Reed and F. Weinhold, *J. Chem. Phys.*, 1983, **78**, 4066; (*e*) A. E. Reed and F. Weinhold, *J. Chem. Phys.*, 1983, **78**, 1736; (*f*) A. E. Reed, R. B. Weinstock and F. Weinhold, *J. Chem. Phys.*, 1985, **83**, 735; (*g*) A. E. Reed, L. A. Curtiss and F. Weinhold, *Chem. Rev.*, 1988, **88**, 899; (*h*) F. Weinhold and J. E. Carpenter, *The Structure of Small Molecules and Ions*, Plenum, New York, 1988, p. 227.
29 K. B. Wiberg, *Tetrahedron*, 1968, **24**, 1083.
30 (*a*) C. Peng, P. Y. Ayala, H. B. Schlegel and M. J. Frisch, *J. Comput. Chem.*, 1996, **17**, 49; (*b*) C. Peng and H. B. Schlegel, *Isr. J. Chem.*, 1994, **33**, 449.
31 (*a*) R. Ditchfield, W. J. Hehre and J. A. Pople, *J. Chem. Phys.*, 1971, **54**, 724; (*b*) W. J. Hehre, R. Ditchfield and J. A. Pople, *J. Chem. Phys.*, 1972, **56**, 2257; (*c*) P. C. Hariharan and J. A. Pople, *Mol. Phys.*, 1974, **27**, 209; (*d*) M. S. Gordon, *Chem. Phys. Lett.*, 1980, **76**, 163; (*e*) P. C. Hariharan and J. A. Pople, *Theor. Chim. Acta*, 1973, **28**, 213.
32 (*a*) J. S. Binkley, J. A. Pople and W. J. Hehre, *J. Am. Chem. Soc.*, 1980, **102**, 939; (*b*) M. S. Gordon, J. S. Binkley, J. A. Pople, W. J. Pietro and W. J. Hehre, *J. Am. Chem. Soc.*, 1982, **104**, 2797; (*c*) W. J. Pietro, M. M. Francl, W. J. Hehre, D. J. Defrees, J. A. Pople and J. S. Binkley, *J. Am. Chem. Soc.*, 1982, **104**, 5039; (*d*) K. D. Dobbs and W. J Hehre, *J. Comput. Chem.*, 1986, **7**, 359; (*e*) K. D. Dobbs and W. J. Hehre, *J. Comput. Chem.*, 1987, **8**, 861; (*f*) K. D. Dobbs and W. J. Hehre, *J. Comput. Chem.*, 1987, **8**, 880.
33 A. W. Ehlers, M. Böhme, S. Dapprich, A. Gobbi, A. Höllwarth, V. Jonas, K. F. Köhler, R. Stegmann, A. Veldkamp and G. Frenking, *Chem. Phys. Lett.*, 1993, **208**, 111.
34 S. H. Vosko, L. Wilk and M. Nusair, *Can. J. Phys.*, 1980, **58**, 1200.
35 (*a*) L. Versluis and T. Ziegler, *J. Chem. Phys.*, 1988, **88**, 322; (*b*) L. Fan and T. Ziegler, *J. Chem. Phys.*, 1991, **95**, 7401.
36 A. D. Becke, *J. Chem. Phys.*, 1987, **88**, 1053.
37 (*a*) J. P. Perdew, *Phys. Rev. B*, 1986, **33**, 8822; (*b*) J. P. Perdew, *Phys. Rev. B*, 1986, **34**, 7406.
38 E. van Lenthe, A. Ehlers and E.-J. Baerends, *J. Chem. Phys.*, 1999, **110**, 8943.
39 (*a*) R. Hoffmann, *J. Chem. Phys.*, 1963, **39**, 1397; (*b*) R. Hoffmann and W. N. Lipscomb, *J. Chem. Phys.*, 1962, **36**, 2179.
40 C. Mealli and D. M. Proserpio, *J. Chem. Educ.*, 1990, **67**, 39.
41 J. H. Ammeter, H.-J. Bürgi, J. C. Thibeault and R. Hoffmann, *J. Am. Chem. Soc.*, 1978, **100**, 3686.